NEGATIVE COUPLING INSTABILITY AND GRANDUNIFIED BARYOGENESIS

TOMISLAV PROKOPEC

Newman Laboratory of Nuclear Studies, Cornell University, Ithaca, NY 14853-5001

In this talk I review my recent work with Brian Greene and Thomas Roos [1]. First I discuss the effect of a negative cross-coupling on the inflaton decay in two scalar field theories. Our main finding is a new effect, the *negative coupling instability,* which leads to explosive particle production and very fast inflaton decay. Then I discuss the consequences of this instability for grandunified baryogenesis models. The novel aspect of this review is an intuitive explanation of the *negative coupling instability,* using field trajectories in the configuration space.

1 Introduction

The problem of the inflaton decay and the subsequent Universe reheat has received a lot of attention in recent years. At this conference an extensive discussion has been devoted to this problem (see talks by D. Boyanovsky and S. Yu. Khlebnikov)[a].

A very brief history of the problem of the inflaton decay is as follows. In 1990 Traschen and Brandenberger [2] discovered that the inflaton, when it starts oscillating after inflation, decays exponentially fast via parametric resonance. The inflaton decays in a few dozens oscillations, which is typically many orders of magnitude faster than the perturbative decay rate [3]. An example is the inflaton decay via a quartic coupling $g\phi^2\chi^2/2$ to a second scalar field χ. The tree-level decay rate is simply

$$\Gamma(\phi\phi \to \chi\chi) = \frac{g^2\Phi^2}{8\pi\omega_\phi}\,, \tag{1}$$

where Φ is the inflaton amplitude, and ω_ϕ its frequency. Since typically $g\Phi \ll \omega_\phi$, the decay time $\tau_{\rm decay} \sim \Gamma^{-1}$ is many orders of magnitude greater than the expansion time $t_H \sim 1/H \sim 1/\omega_\phi$.

[a] Daniel Boyanovsky presented a new inflationary scenario in which the classical limit gives an accurate description of the problem. Sergei Khlebnikov argued that generically, in theories with weak couplings, the classical limit is reached when "occupation numbers" of the field modes become large.

2 Parametric resonance in a toy model: the Mathieu equation

Consider the simple two field case with the potential:

$$V(\phi,\chi) = \frac{1}{2}m_\phi^2\phi^2 + \frac{g}{2}\chi^2\phi^2 \,. \tag{2}$$

In a static universe the linearized mode equations for χ can be written as the Mathieu equation

$$\frac{d^2\chi_k}{dz^2} + \left[A(k) - 2q\cos(2z)\right]\chi_k = 0\,, \tag{3}$$

$$A(k) = \frac{\omega_\chi(k)^2}{(\omega_\phi)^2} + 2q\,, \qquad q = \frac{g\Phi^2}{4(\omega_\phi)^2}\,, \tag{4}$$

where $z = \omega_\phi t$, and $\omega_\chi(k)^2 = k^2 + m_\chi^2$ is the frequency squared of χ_k. The instability chart of the Mathieu equation is depicted in figure 1. The $\mu = 0$ curves divide the chart into stable and unstable regions. For $g > 0$, $A \geq 2|q|$, and $\mu_{\max} \leq 0.3$, as can be seen in figure 1. One can define μ as follows: the amplitude of the corresponding mode grows in one oscillation of the inflaton ϕ by a factor $\exp 2\pi\mu$. Since the mode occupation numbers grow as the amplitude squared, this growth can be interpreted as particle production, and is termed *parametric resonance.* On the other hand for $g < 0$, $A \geq -2|q|$, and one can show [1] that $\mu \leq 4|q|^{1/2}/\pi$, which can be $\gg 1$ when $|q| \gg 1$. This phenomenon is what we mean by the *negative coupling instability.* The question is can this instability occur in a natural physical setting?

3 Parametric resonance in a realistic model

To understand this question, consider the general renormalizable two scalar field potential with a $\mathcal{Z}_2 \times \mathcal{Z}_2$ global symmetry

$$V(\phi,\chi) = \frac{1}{2}m_\phi^2\phi^2 + \frac{1}{2}m_\chi^2\chi^2 + \frac{\lambda_\phi}{4}\phi^4 + \frac{\lambda_\chi}{4}\chi^4 + \frac{g}{2}\phi^2\chi^2 \tag{5}$$

in an expanding universe. The results I discuss in this section are obtained numerically in [1]. Assume a natural hierarchy of couplings (1) $\lambda_\chi > g > \lambda_\phi$ (when $g > 0$), and (2) $\lambda_\chi > |g| > \lambda_\phi$, $r \equiv \lambda_\phi\lambda_\chi/g^2 > 1$ (when $g < 0$). In the former case the inflaton ϕ rolls down in inflation and then oscillates along the $\chi = 0$ direction, leading to the standard growth of the resonant modes (in the χ direction). As a consequence, the inflaton amplitude Φ decays exponentially fast into the χ fluctuations with the decay time of order

$$\tau_{\rm decay} \simeq \frac{1}{2\mu\omega_\phi}\ln\frac{n_{\max}}{n_0}\,, \qquad \mu \leq 0.3 \tag{6}$$

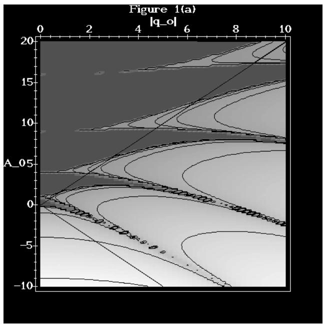

Figure 1: The stability chart for the Mathieu equation. The dark regions are stable. In the unstable (light) regions we marked contours of constant instability index μ. The contours shown are $\mu = 0, 0.1, 0.2, 0.3, 0.5, 1, 2, 3$. The lines $A = \pm 2|q|$ are also plotted.

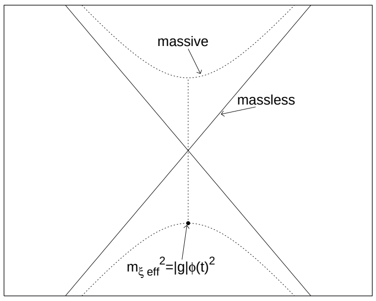

Figure 2: The valleys of the potential (5). In the massless case oscillations are along $\chi_0(t)/\phi_0(t) = \tan\Theta = \pm(-g/\lambda_\chi)^{1/2}$, while in the massive case the trajectories are given by (7).

where $n_{\rm max} \sim 1/g$ and $n_0 \simeq 1/2$ are the maximum and initial occupation numbers, respectively, and ω_ϕ is the frequency of ϕ at the end of inflation.

When $g < 0$, the *valley* of the potential (5) is not any more along the $\chi = 0$, but along

$$\tilde{\chi}_0^2 = \begin{cases} \frac{-m_\chi^2 - g\phi_0^2}{\lambda_\chi} & \text{for} \quad m_\chi^2 + g\phi_0^2 < 0 \\ 0 & \text{otherwise} \end{cases} \quad . \tag{7}$$

If $\chi_0 \approx \tilde{\chi}_0$ initially, then it remains so during inflation (as long as $|q| \gg 1/10$). More generally, the valley (7) is the attractor for the zero mode. However, during inflation the superhorizon modes grow (to generate seeds for structure formation, just like in ordinary inflationary theories). On figure 2 we show the valleys of the potential both for $m_\chi^2 = 0$ and $m_\chi^2 > 0$. In the former case the valley trajectories are defined by $\chi_0(t)/\phi_0(t) \equiv \tan\Theta = \pm(-g/\lambda_\chi)^{1/2}$, and one can easily show that along the valley directions the initial stages of the evolution look just like the positive g case with $q_{\rm eff} = 2|q|$ and $\mu_{\rm eff} \leq 0.3$. Indeed, we observe this behavior in our numerical simulations. However, at certain point the backreaction effects from created particles become important: the χ excitations become massive with $m_{\chi\ \rm eff}^2 = m_\chi^2 + 3\lambda_\chi\langle\chi^2\rangle + g\langle\phi^2\rangle$, and the picture changes dramatically. The valley equation obeys (7) so that for $m_{\chi\ \rm eff}^2 = |g|\phi(t)^2$ the valley has a characteristic curved shape as seen in figure 2. If at this time $\phi(t)$ is growing, and χ has a small oscillating amplitude whose phase matches onto the decaying solution, then $\{\phi(t), \chi(t)\}$ does not follow the

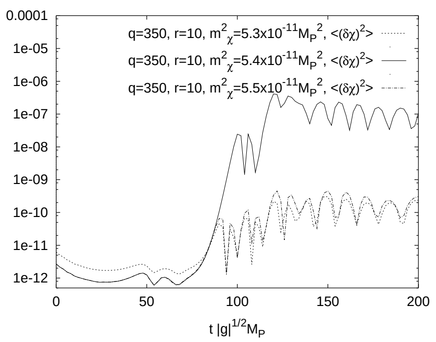

Figure 3: The χ field variances for three runs with slightly different χ masses ($m_\phi^2 = 7.2 \times 10^{-13} M_{\rm P}^2$, $\lambda_\phi = 10^{-12}$, $\lambda_\chi = 10^{-5}$, $g = -10^{-9}$)

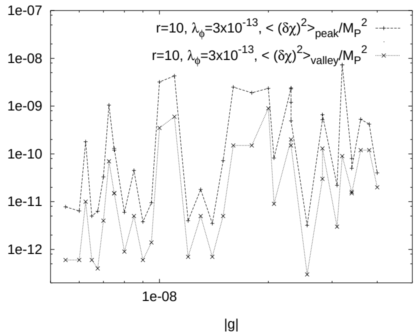

Figure 4: Maximum peak and valley variances as a function of $|g|$ for $m_\chi = 10^{14}$GeV. The inflaton is massless ($m_\phi = 0$), $\lambda_\phi = 3 \times 10^{-13}$, $g < 0$ and λ_χ is adjusted to keep $r = 10$.

valley in (7) but instead it climbs the ridge. Consequently, the infrared χ modes "see" an inverted harmonic oscillator and their amplitude grows exponentially fast. This is what we mean by the *negative coupling instability.* In this case the mode amplitudes and field variances grow typically much faster than in the case of parametric resonance. Indeed, in our numerical simulations we observe the instability exponent $\mu \leq |q|^{1/2}$ for $|q| \gg 1$. This instability occurs generically when $\Phi^2 \geq m_{\chi\,\rm eff}^2 \geq |q|^{1/2}\omega_\phi^2$, and hence even in the massless χ case due to the backreaction effects. Note the stochastic nature of the instability. In order to predict how each of the modes behaves, one must be able to compute the phase of χ_0 at $|g|\phi^2(t) = m_{\chi\,\rm eff}^2$ very accurately. This sensitivity is illustrated in figure 3, in which we show the dramatic change in the variance growth, when the χ mass changes by a tiny amount. For example, when $|q| = 350$, $\Delta m_\chi / m_\chi \simeq \pm 0.01$ leads to a change in the variance growth by a factor $\sim 10^3$. The instability peaks at $m_\chi^2 = 5.5 \times 10^{-11} M_{\rm P}^2$ for which $\mu_{\rm max} \simeq 20 \simeq |q|^{1/2}$. Note that similar instability occurs when $m_\chi^2 < 0$, $g > 0$. In this case an investigation of the configuration space indicates that the instability occurs quite generically. Indeed, if at the end of inflation $\phi_0^2 \gg -m_\chi^2/g$ and χ is sufficiently close to the valley value at $\chi_0 = 0$, once $\phi_0(t)^2 < -m_\chi^2/g$ the infrared χ modes become unstable, leading to rapid mode growth and particle production.

Without going into details, we now summarize the consequences of the negative coupling instability: (1) the inflaton decays much faster, typically within a few oscillations (with $\langle\mu\rangle \sim 0(1)$); (2) as a consequence of the following relation $A \geq 2|q| + |q|^{1/2}$, which specifies when the resonance shuts down, the field variances grow larger than in the positive g case by a factor $\sim 4|q|^{1/2}$, and hence have a much stronger symmetry restoring force; (3) massive χ particles are produced much easier, which may be relevant for grandunified baryogenesis (see below), and the unstable momenta are of a much broader range ($\Delta k^2 \sim |g|\Phi^2 - m_\chi^2$).

4 Baryogenesis and the negative coupling instability

In this section I discuss how the negative coupling instability can be used to facilitate grandunified baryogenesis. I first summarize some of the results concerning production of heavy particles, and then, on an example of a simple toy model, I discuss how this heavy particle production can affect grandunified baryogenesis.

For a realistic choice of couplings, which is in chaotic inflationary models constrained by the COBE satellite measurements to be $\lambda_\phi \approx 3 \times 10^{-13}$ or $m_\phi \leq 2 \times 10^{13}$GeV, one can produce massive particles with $m_\chi \sim 10^{14}$GeV (as typically required by GUT baryogenesis models), provided $|g| \geq 10^{-8}$ and $\lambda_\chi > 3 \times 10^{-4}$ (for stability), see figure 4, which corresponds to the parameter space $10^{-6} \geq |g| \geq 10^{-8}$, $1 > \lambda_\chi > 3 \times 10^{-4}$, leaving plenty of opportunity for baryogenesis model building. This is to be contrasted with the positive g case for which $g \geq 10^{-3}$ is required. Such a large value leads to an unpleasant fine tuning problem since the small value of λ_ϕ needs to be protected against radiative corrections.

To obtain an estimate of the baryon asymmetry that could be produced during preheating we study a simple toy model [5]. In short, the model can be described as follows. Initially a certain amount of energy is transferred from the inflaton to a heavy GUT scalar field *via* nonperturbative mechanisms, an example of which is the negative coupling instability. The result is a cold (far from equilibrium) fluid of massive particles (with a mass M_χ), which we assume decays in a B and CP violating manner into light degrees of freedom that instantly thermalize. This out-of-equilibrium CP violating decay is the crucial step that leads to net baryon production. In order to treat the problem analytically we further assume that at all times the temperature T of the light relativistic particles is $\ll M_\chi$. The main results of this investigation are expressions for the final baryon-to-entropy ratios n_B/s for a massless and massive inflaton. Here we quote the result for the massless inflaton decay

$$\frac{n_B}{s} = \epsilon \left(\frac{\rho_X^0}{g_* M_X^4}\right)^{\frac{1}{4}} \left(\frac{\Gamma_X}{H_0}\right)^{\frac{3}{4}} , \quad \text{when} \quad \rho_\phi^0 \Gamma_\chi, \rho_\phi^0 \Gamma_\chi < g_* M_\chi^4 H_0 , \qquad (8)$$

where ϵ an effective CP violation (the decay of each pair $X - \bar{X}$ produces

ϵ baryons), ρ_ϕ^0 and ρ_X^0 are the initial energy densities of the X and ϕ fluid, respectively, $g_* \sim 10^2 - 10^3$ is the number of relativistic degrees of freedom, M_X is the mass of X, Γ_ϕ, Γ_X are the decay rates for ϕ and X, respectively, and H_0 is the expansion rate. In addition we have assumed a "natural" hierarchy of time scales $H_0 \gg \Gamma_\chi \gg \Gamma_\phi$. The remarkable feature of this result is that the final baryon-to-entropy ratio does not depend on the decay constants Γ_X and Γ_ϕ. Why this is so can be understood as follows. As long as the temperature never rises close to M_X so that the massive particles X are never re-populated by scattering off the radiation fluid, most of the massive particles decay out of equilibrium and create $\simeq \epsilon N_\chi^0$ baryons, independent on the decay rate Γ_χ. The entropy production, if dominated by the late inflaton decay, is also independent on the decay rate Γ_ϕ, so that the final baryon-to-entropy ratio is independent on the decay rates. We believe that this feature lends more credibility to our result.

According to (8) the final baryon to entropy ratio is proportional to ρ_X^0. Since the energy density of the (non-relativistic) X particles is proportional to their variance ($\rho_X \approx M_X^2 \langle(\delta X)^2\rangle$), the spikes in figure 4 are directly imaged to spikes in baryon production. For a massless inflaton the final baryon to entropy ratio is expressed in terms of the maximum variance

$$\frac{n_B}{s} = \epsilon g_*^{-\frac{1}{4}} \left(\frac{4g^2}{\lambda_\phi}\right)^{\frac{3}{4}} \frac{\langle\left(\delta X^2\right)^2\rangle_0}{M_X^2}\,, \tag{9}$$

From figure 4 we see that the largest value for the variance $\langle\left(\delta X^2\right)^2\rangle_0 \sim 10^{-9} M_{\rm P}^2$, where $M_{\rm P} \simeq 2.4 \times 10^{18}$GeV is the reduced Planck mass, leading to a maximum value for the baryon-to-entropy ratio $n_B/s \sim 10^{-3}\epsilon$ (we set $g_* = 100$). We conclude that with our toy model it is not hard to obtain baryon-to-entropy ratio consistent with observation $n_B/s \sim 2 - 12 \times 10^{-11}$. Certainly more realistic models for GUT baryogenesis at preheating will have to be constructed to verify the viability of this scenario, but the preliminary results are very promising.

Acknowledgements

This research was conducted using the resources of the Cornell Theory Center, which receives major funding from the National Science Foundation (NSF) and New York State, with additional support from the Advanced Research Projects Agency (ARPA), the National Center for Research Resources at the National Institutes of Health (NIH), IBM Corporation, and other members of the center's Corporate Partnership Program. Writing this review would not be possible without the contribution of Brian Greene and Thomas Roos. I acknowledge NSF funding.

References

1. B. R. Greene, T. Prokopec, and T. G. Roos, to be published in *Phys. Rev.* D (1997), hep-ph/9705357.
2. J. H. Traschen and R. H. Brandenberger, *Phys. Rev.* D **42**, 2491 (1990).
3. A. A. Starobinskii, in *Quantum Gravity, Proceedings of the Second Seminar "Quantum Theory of Gravity"* (Moscow, 13 - 15 Oct. 1981), eds. M. A. Markov ad P. C. West (Plenum, New York, 1984), p. 103; A. Dolgov and A. Linde, *Phys. Lett.* B **116**, 329 (1982); L. F. Abbott, E. Farhi, and M. Wise, *Phys. Lett.* B **117**, 29 (1982).
4. L. Kofman, A. D. Linde and A. A. Starobinskii, *Phys. Rev. Lett.* **73**, 3195 (1994).
5. E. W. Kolb, A. Linde, and A. Riotto, *Phys. Rev. Lett.* **77**, 4290 (1996).